Stability control of electric vehicles based on a novel longitudinal force distribution strategy and Smith predictor

HUAN SHEN*, YUNSHENG TAN, MANHONG HUANG
College of Energy and Power Engineering
Nanjing University of Aeronautics and Astronautics
29 Yudao St., Nanjing 210016
CHINA
*Corresponding author: huan_shen@nuaa.edu.cn

Abstract: In this paper, a novel yaw moment control system is proposed to improve vehicle's handling and stability. The control system includes reference model, DYC controller, Distributer, and Smith predictor. The reference model is used to obtain the desired yaw rate. The DYC controller determines the desired yaw moment by means of sliding-mode technique. The Distributer, based on maneuverability and comfort, distributes driving torque or braking torque according to the desired yaw rate. The Smith predictor based on linear vehicle model is used to solve the time delay problems caused by actuators and sensors/observers. The simulation results show that the proposed control algorithm can improve vehicle's handling and stability effectively.

Key-Words: Electric vehicles; Drive force distribution; Longitudinal force distribution; Sliding mode Control; DYC

1 Introduction

With energy crisis, environmental deterioration and breakthroughs in battery technology, electric vehicles have recently emerged and become a research hotspot. The in-wheel motor electric vehicle with unique advantages, as one form of electric vehicles, has become the mainstream of current electric vehicles' research fields [1-2]. Researchers have studied the problems of stability on the in-wheel motor [3-4].

Direct yaw moment control (DYC) and active steering control (ASC) are the two types of well-known electronic stability control technologies which are used to solve stability problems of the vehicle [5-6]. Compared with ASC, DYC has proved its superiority on improving vehicles' handling and stability [7-9]. DYC stabilizes the vehicle yaw motion and increases vehicle maneuverability by applying differential longitudinal forces between the inner and outer wheels. In traditional vehicles, DYC is mainly achieved through differential braking types. However, this approach with a strong active intervention will cause the change of longitudinal forces, violate the driver's intention, and affect vehicle driving comfort [10-11]. The in-wheel motor electric vehicle can realize the control alone of the four in-wheel motors. Therefore, DYC can be achieved through a variety of methods, such as driving, braking, and both.

In this paper, the stability problems of the in-wheel motor electric vehicle are studied by means of the direct yaw moment control. A novel yaw moment control system is proposed, including reference model, DYC controller, Distributer, and Smith predictor. The reference model is used to obtain the desired yaw rate. The DYC controller calculates the additional yaw moment to realize the tracking of desired yaw rate. Based on the distribution strategy of maneuverability and comfort, the Distributer distributes driving torque or braking torque in order to achieve the yaw moment. However, when the in-wheel motors apply driving torque or braking torque to tyres, the time delay of motors will have a bad influence on the stability of the control system. Thus, the Smith predictor based on linear vehicle model is designed to solve the time delay problems in the control process. Finally, combined with a nonlinear vehicle model, extensive simulation researches are reported in order to show effectiveness of the proposed algorithm.

The rest of this paper is organized as follows. Section 2 addresses the vehicle dynamic model and a nonlinear tyre model. Section 3 presents the proposed control system in details, including the reference model, DYC controller, Distributer, and Smith predictor. The simulation results are shown and discussed in Section 4. Finally, the conclusion is reached in Section 5.

2 The vehicle and the tyre models

2.1 The vehicle model

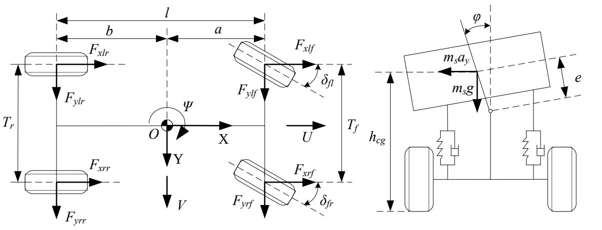

Fig. 1: SAE 8DOF Vehicle model

The standard coordinate system defined by Society of Automotive Engineers (SAE) as in Fig. 1 is used in this paper. And a vehicle model with 8 degrees of freedom is established [7, 12-13], which includes longitudinal and lateral motions (U, V), yaw motion (r), and body roll motion of the vehicle (p), as well as the four wheels' rotational motion (w_{fl}, w_{fr}, w_{rl}, w_{rr}). Here, the vertical and pitch motions are neglected. Then the governing equations of motion for the 8DOF nonlinear dynamic vehicle model can be expressed as follows:

$$m\dot{U} = mVr + F_{xfl} + F_{xfr} + F_{xrl} + F_{xrr} \tag{1}$$

$$m\dot{V} = -mUr - m_s e\dot{p} + F_{yfl} + F_{yfr} + F_{yrl} + F_{yrr} \tag{2}$$

$$\begin{aligned} I_z\dot{r} &= I_{xz}\dot{p} + a\left(F_{yfl} + F_{yfr}\right) - b\left(F_{yrl} + F_{yrr}\right) \\ &+ \frac{T_f}{2}\left(F_{xfl} - F_{xfr}\right) + \frac{T_r}{2}\left(F_{xrl} - F_{xrr}\right) + M_z \end{aligned} \tag{3}$$

$$I_x\dot{p} = -m_s e\dot{V} + I_{xz}\dot{r} - m_s eUr + m_s ge\sin\varphi - K_\varphi\varphi - C_\varphi\dot{\varphi} \tag{4}$$

$$\dot{\varphi} = p \tag{5}$$

$$I_w\dot{\omega}_i = -R_w F_{ti} + T_i \quad \text{with } i = fl, fr, rl, rr \tag{6}$$

In the above equations, m stands for the total mass of the vehicle, m_s is the sprung mass. U is the longitudinal vehicle velocity, V is the lateral vehicle velocity, r is the yaw rate, φ is the roll angle, p is the roll rate. F_{xi} and F_{yi} stand for the tyre force components in the x and y directions, respectively. a and b are the distances from the centre of gravity to the front and rear axles, respectively. T_f and T_r are the front and rear track width, respectively. e is the distance between the center of gravity of the sprung mass and the roll centre. I_z and I_x are yaw inertia moment and roll inertia moment, respectively. I_{xz} is sprung mass product of inertia. I_w is wheel moment of inertia, R_w is wheel radius, w_i is wheel rotational speed. T_i is the driving torque or the braking torque applied to the wheel. K_φ and C_φ are roll stiffness and roll damping, respectively.

The tyre forces F_{xi} and F_{yi} can be deduced through the coordinate transformation:

$$F_{xi} = F_{ti}\cos\delta_i - F_{si}\sin\delta_i \quad \text{with } i = fl, fr, rl, rr \tag{7}$$

$$F_{yi} = F_{ti}\sin\delta_i + F_{si}\cos\delta_i \quad \text{with } i = fl, fr, rl, rr \tag{8}$$

where, F_{ti} and F_{si} are the tractive and the lateral tyre forces, respectively. δ_i is the steering angle, the rear wheel angle is zero, namely $\delta_{rl}=\delta_{rr}=0$.

Considering the load transfer caused by longitudinal and lateral accelerations, the nominal vertical load of each wheel can be expressed as follows:

$$F_{zfl} = \frac{mg}{2}\left[\frac{b}{l} - \frac{\left(\dot{U} - Vr\right)h_{cg}}{gl} + K_R\left(\frac{h_{cg}a_y}{T_f g} - \frac{m_s e}{mT_f}\sin\varphi\right)\right] \tag{9}$$

$$F_{zfr} = \frac{mg}{2}\left[\frac{b}{l} - \frac{\left(\dot{U} - Vr\right)h_{cg}}{gl} - K_R\left(\frac{h_{cg}a_y}{T_f g} - \frac{m_s e}{mT_f}\sin\varphi\right)\right] \tag{10}$$

$$F_{zrl} = \frac{mg}{2}\left[\frac{a}{l} + \frac{\left(\dot{U} - Vr\right)h_{cg}}{gl} + \left(1 - K_R\right)\left(\frac{h_{cg}a_y}{T_r g} - \frac{m_s e}{mT_r}\sin\varphi\right)\right] \tag{11}$$

$$F_{zrr} = \frac{mg}{2}\left[\frac{a}{l} + \frac{\left(\dot{U} - Vr\right)h_{cg}}{gl} - \left(1 - K_R\right)\left(\frac{h_{cg}a_y}{T_r g} - \frac{m_s e}{mT_r}\sin\varphi\right)\right] \tag{12}$$

where, $l = a + b$ is wheelbase, h_{cg} is the height of center of sprung gravity, $K_R = K_f/(K_f + K_r)$, K_f and K_r are the front and rear roll stiffness.

The vehicle-to-global coordinate transformations can be expressed as follows:

$$\dot{X} = U\cos\psi - V\sin\psi \tag{13}$$

$$\dot{Y} = -U\sin\psi - V\cos\psi \tag{14}$$

where, ψ is the yaw angle.

2.2 The tyre model

In the paper, the Dugoff model [14] is used to calculate the longitudinal and lateral forces on the tyres. According to 8DOF model, each wheel has an independent slip angle:

$$\alpha_{fl} = \delta_{fl} - \arctan\left(\frac{V + ar}{U + 0.5T_f r}\right) \tag{15}$$

$$\alpha_{fr} = \delta_{fr} - \arctan\left(\frac{V + ar}{U - 0.5T_f r}\right) \tag{16}$$

$$\alpha_{rl} = \arctan\left(\frac{br - V}{U + 0.5T_r r}\right) \tag{17}$$

$$\alpha_{rr} = \arctan\left(\frac{br - V}{U - 0.5T_r r}\right) \tag{18}$$

Moreover, the longitudinal tyre slip is defined as follows:

$$S_i = \begin{cases} \dfrac{R_w\omega_i - u_i}{u_i}, & R_w\omega_i < u_i \\ \dfrac{R_w\omega_i - u_i}{R_w\omega_i}, & R_w\omega_i \geq u_i \end{cases} \quad \text{with } i = fl, fr, rl, rr \tag{19}$$

where, u_i is the longitudinal velocity of each wheel:

$$u_{fl} = \left(U + \frac{1}{2}T_f r\right)\cos\delta_{fl} + \left(V + ar\right)\sin\delta_{fl} \tag{20}$$

$$u_{fr} = \left(U - \frac{1}{2}T_f r\right)\cos\delta_{fr} + \left(V + ar\right)\sin\delta_{fr} \tag{21}$$

$$u_{rl} = U + T_r r/2 \tag{22}$$
$$u_{rl} = U - T_r r/2 \tag{23}$$

Neglecting the self-aligning moment, the tractive force F_{ti} and the lateral force F_{si} are determined by the following equations:

$$F_{ti} = \frac{C_i S_i}{1 - S_i} f(\lambda) \tag{24}$$

$$F_{si} = \frac{C_\alpha \tan\alpha_i}{1 - S_i} f(\lambda) \tag{25}$$

$$f(\lambda) = \begin{cases} \lambda(2-\lambda) & \text{if } \lambda < 1 \\ 1 & \text{if } \lambda \geq 1 \end{cases} \tag{26}$$

$$\lambda = \frac{\mu F_{zi}\left[1 - \varepsilon_r u_i \sqrt{S_i^2 + \tan^2\alpha_i}\right](1 - S_i)}{2\sqrt{C_i^2 S_i^2 + C_\alpha^2 \tan^2\alpha_i}} \tag{27}$$

where, μ is nominal friction coefficient between tyre and ground, ε_r is road adhesion reduction factor, C_i and C_α are longitudinal stiffness and cornering stiffness of the tyre, respectively.

2.3 Linear 2DOF vehicle model

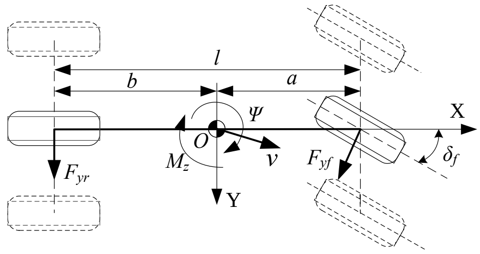

Fig. 2: 2DOF vehicle model

In this paper, the controller design uses linear two degree-of-freedom (2DOF) vehicle model as reference model (as shown in Fig. 2), which includes lateral motion and yaw motion. The velocity of vehicle is assumed to be unchanged. 2DOF vehicle model can describe the main handling characteristics of vehicle in linear range very well [15]. The differential equations are as follows:

$$\dot{\beta} = -\frac{C_f + C_r}{mv}\beta - \left(1 + \frac{C_f a - C_r b}{mv^2}\right)r + \frac{C_f}{mv}\delta_f \tag{28}$$

$$\dot{r} = \frac{C_r b - C_f a}{I_z}\beta - \frac{C_f a^2 + C_r b^2}{I_z v} r + \frac{C_f a}{I_z}\delta_f + \frac{1}{I_z} M_z \tag{29}$$

where, C_f and C_r are cornering stiffness of front and rear tyres, respectively. v is the velocity of vehicle mass center, β is the slip angle of vehicle, δ_f and δ_r are the front and rear steering angle, respectively.

The output vector is $\mathrm{X} = [\beta \quad r]^{\mathrm{T}}$, the input vector is $u = \left[\delta_f \quad M_z\right]^{\mathrm{T}}$, then the matrix form of 2 DOF linear vehicle model can be given by

$$\dot{\mathrm{X}} = \mathrm{AX} + \mathrm{B}u \tag{30}$$

where,

$$\mathrm{X} = \begin{bmatrix} \beta \\ r \end{bmatrix}, \qquad \mathrm{A} = \begin{bmatrix} -\dfrac{C_f + C_r}{mv} & -1 - \dfrac{C_f a - C_r b}{mv^2} \\ -\dfrac{C_f a - C_r b}{I_z} & -\dfrac{C_f a^2 + C_r b^2}{I_z v} \end{bmatrix}$$

$$\mathrm{B} = \begin{bmatrix} \dfrac{C_f}{mv} & 0 \\ \dfrac{C_f a}{I_z} & \dfrac{1}{I_z} \end{bmatrix}, \qquad \mathrm{u} = \begin{bmatrix} \delta_f \\ M_z \end{bmatrix}$$

3 Control System Design

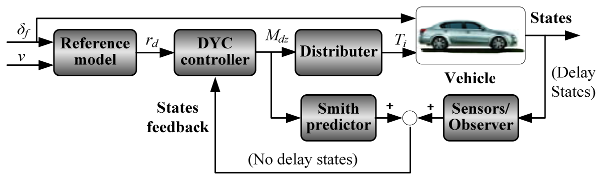

Fig. 3: Structure of the control system

The control system scheme adopted in this paper is shown in Fig. 3, which includes reference model, DYC controller, Distributer, and Smith predictor and so on. Here, the reference model is calculated to get the desired yaw rate r_d, which is as the tracking target of the control system. DYC controller is designed to calculate the yaw moment M_z, which is used to track the desired yaw rate r_d. Distributer is used to calculate the driving and braking torque of tyres to meet the demand of the yaw moment M_z. In order to improve stability margin of the control system, Smith predictor is used to solve the delay problem of actuators.

3.1 Reference Model

The role of the reference model is to calculate the response of the yaw rate in line with drivers' habits, and provides the tracking target for the DYC controller. In this paper, 2 DOF vehicle model is as the reference model. Therefore, the steady-state yaw rate response of the reference model can be described as follows:

$$r = \frac{v}{l + K_v v^2}\delta_f \tag{31}$$

where K_v is the vehicle understeer gradient [5], which is defined as:

$$K_v = \frac{m}{l}\left(\frac{b}{C_f} - \frac{a}{C_r}\right) \tag{32}$$

Since the yaw rate is constricted by road adhesion conditions, the maximum values of the yaw rate are related to road adhesion coefficient and velocity of vehicle [5]:

$$|r| \leq |r_{\max}| = 0.85\frac{\mu \cdot g}{v} \tag{33}$$

Hence, the desired yaw rate can be amended as:

$$r^* = \min\left\{\left|\frac{v}{l + K_v v^2}\delta_f\right|,\ \left|0.85\frac{\mu \cdot g}{v}\right|\right\} \cdot \mathrm{sgn}(\delta_f) \quad (34)$$

In order to avoid the transient response of yaw rate with great oscillation or overshoot, we need to use the first-order filter to filter the desired yaw rate r^* in practical process. Therefore, the ultimate desired tracking yaw rate r_d as the controller input is

$$r_d = \min\left\{\left|\frac{v}{l + K_v v^2}\delta_f\right|,\ \left|0.85\frac{\mu \cdot g}{v}\right|\right\} \cdot \mathrm{sgn}(\delta_f) \cdot \frac{1}{1+\tau_r s} \quad (35)$$

where τ_r is the delay time of yaw rate, whose range is 0.1~0.25s.

3.2 DYC Controller Design

According to the vehicle feedbacks, the DYC controller calculates the additional yaw moment which is required for tracking the reference model so as to realize the tracking of desired yaw rate r_d. In order to simplify the structure of the DYC controller and facilitate the design of Smith predictor, DYC controller is designed by sliding-mode technique according to 2DOF vehicle model in this paper.

In order to decrease tracking errors further, this paper introduces an integral operator in the sliding mode design as follows:

$$S = \dot{e} + c_0 e + c_1 \int e \mathrm{d}t \quad (36)$$

where $\dot{e}$ is the tracking error of yaw rate, $\dot{e} = r - r_d$, c_0 and c_1 are the tuning parameters.

Then,

$$\dot{S} = \ddot{e} + c_0\dot{e} + c_1 e = \dot{r} - \dot{r}_d + c_0\dot{e} + c_1 e \quad (37)$$

Combining Equation (29) with (37), and using the constant converging velocity, namely, $\dot{S} = -K \cdot \mathrm{sgn}(S)$, $K > 0$, then

$$\dot{S} = \frac{C_r b - C_f a}{I_z}\beta - \frac{C_f a^2 + C_r b^2}{I_z v} r + \frac{C_f a}{I_z}\delta_f + \frac{1}{I_z}M_z - \dot{r}_d + c_0\dot{e} + c_1 e = -K \cdot \mathrm{sgn}(S) \quad (38)$$

$$u = M_z = I_z\left(-\frac{C_r b - C_f a}{I_z}\beta + \frac{C_f a^2 + C_r b^2}{I_z v} r - \frac{C_f a}{I_z}\delta_f + \dot{r}_d - c_0\dot{e} - c_1 e - K \cdot \mathrm{sgn}(S)\right) \quad (39)$$

where sgn is sign function, and K is the tuning parameter of the controller which determines the speed of the system slide to the sliding surface S.

To reduce the chattering phenomenon, the sign function in Equation (39) is replaced by the saturation function shown as follows:

$$\mathrm{sat}\left(\frac{S}{\Delta}\right) = \begin{cases} \mathrm{sgn}(S) & |S| \geq \Delta \\ S/\Delta & |S| < \Delta \end{cases}$$

where $\Delta > 0$ is the boundary layer thickness.

Finally, the desired additional yaw moment M_{dz} is

$$M_{dz} = I_z\left(-\frac{C_r b - C_f a}{I_z}\beta + \frac{C_f a^2 + C_r b^2}{I_z v} r - \frac{C_f a}{I_z}\delta_f + \dot{r}_d - c_0\dot{e} - c_1 e - K \cdot \mathrm{sat}(S)\right) \quad (40)$$

3.3 Distributer Design

According to the yaw moment calculated by DYC controller, Distributer realizes the yaw moment control based on driving or braking torque on each wheel. If the lateral force is required to be constant, the change of longitudinal force will cause the change of slip angle of the tyre. Namely, exerting longitudinal force raises the slip angle [10].

Equation (32) can be rewritten as

$$K_v = \frac{1}{a_y}(\alpha_f - \alpha_r) \quad (41)$$

where a_y is the lateral acceleration of the vehicle.

Equation (41) is to show that, if the longitudinal force is exerted on the front wheels, α_f increases, the vehicle tends to understeer; if the longitudinal force is exerted on the rear wheels, α_f decreases, the vehicle tends to oversteer [10]. Meanwhile, in order to reduce the effects of the driving comfort caused by the change of the longitudinal velocity, the demand of longitudinal force remains the same on the premise of meeting the demand of the yaw moment in order to reduce the change of longitudinal velocity due to the change of the longitudinal force. Namely, not only can the distribution of the driving torque and braking torque simultaneously improve the manipulate efficiency, but also it can meet the demand of longitudinal force unchanged. In this paper, the distribution strategy of the differential longitudinal force is developed based on this analysis. Therefore, the distribution strategy is illustrated in Fig. 4.

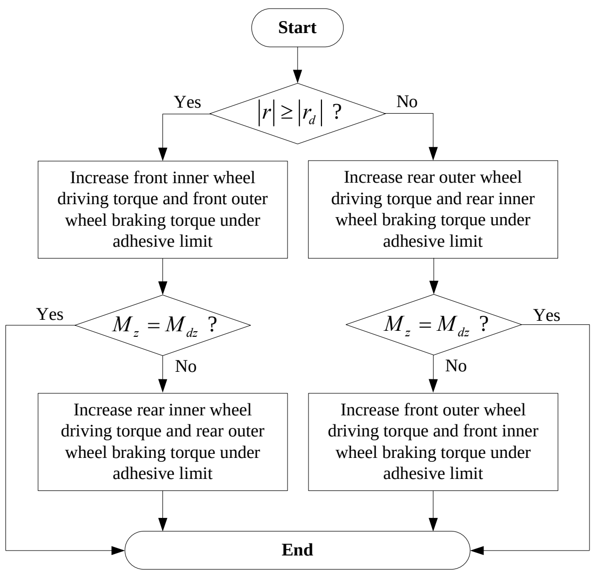

Fig. 4: Longitudinal force distribution strategy

The driving torque and braking torque distributed by Distributer can not directly affect the vehicle, but it works with the help of torques applied on the wheel by actuators, like in-wheel motor. The motors dynamics are modeled as first-order systems with time delay as shown in Equation (42). This paper studies the influence of actuator dynamics on the controller.

$$G_{ai}(s)=\frac{K_a e^{-\vartheta s}}{\tau_a s+1} \quad \text{with } i=fl,fr,rl,rr \tag{42}$$

where K_a is the gain of the motor actuator, ϑ is the pure time delay of motor and also includes the pure time delay of sensors in next section, τ_a is the first-order delay of the motor.

Therefore, the driving torque and braking torque T_i applied on the wheel is

$$T_i=G_{ai}(s)T_i^* \tag{43}$$

In addition, the relationship between the driving torque or braking torque T_i and additional yaw moment M_{dz} is expressed as follow

$$M_{dz}=\frac{T_f}{2}\left(\frac{T_{fl}}{R_w}-\frac{T_{fr}}{R_w}\right)+\frac{T_r}{2}\left(\frac{T_{rl}}{R_w}-\frac{T_{rr}}{R_w}\right) \tag{44}$$

3.4 Smith predictor

As for the design of the controller, the effect of motor delay can not be taken into consideration. Additionally, the motor delay easily leads to the system's instability, especially the pure time delay. Therefore, the study on vehicle stability should involve the delay problem of the actuator and sensor/observer. In this paper, the Smith predictor is designed to solve the pure time delay problem.

The pure time delay of the sensor/observer is included in the item $e^{-\vartheta s}$. The vehicle nonlinear model is too complex to measure and identify conveniently. Therefore, combined with the normal form of the Smith predictor design [17-18], the vehicle nonlinear model is replaced by the linear 2DOF vehicle model to design the Smith predictor. The Smith predictor can be expressed by

$$G_s(s)=G_v(s)\left(1-G_{ai}(s)\right) \tag{45}$$

where $G_v(s)$ is the transfer function of the side slip angle and yaw rate to the yaw moment, and can be obtained by Equation (30)

$$\begin{bmatrix} G_{\beta-\delta_f}(s) & G_{\beta-M_z}(s) \\ G_{r-\delta_f}(s) & G_{r-M_z}(s) \end{bmatrix}=(s\mathrm{I}-\mathrm{A})^{-1}\mathrm{B} \tag{46}$$

$$G_v(s)=\begin{bmatrix} G_{\beta-M_z}(s) \\ G_{r-M_z}(s) \end{bmatrix} \tag{47}$$

4 Simulation Results and Analysis

Table 1 Parameters of vehicle

Parameters	Description	Value
m	Vehicle total mass	1298.9 kg
m_s	Vehicle sprung mass	1167.5 kg
a	Distance of c.g. from the front axle	1 m
b	Distance of c.g. from the rear axle	1.454 m
T_f	Front track width	1.436 m
T_r	Front track width	1.436 m
h_{cg}	Height of the sprung mass c.g.	0.533
e	Distance of the sprung mass c.g. from the roll axes	0.4572 m
I_z	Vehicle moment of inertia about yaw axis	1627 kg·m^2
I_x	Vehicle moment of inertia about roll axis	498.9 kg·m^2
I_{xz}	Sprung mass product of inertia	0 kg·m^2
R_w	Wheel radius	0.35 m
I_w	Wheel moment of inertia	2.1 kg·m^2
C_α	Cornering stiffness of one tyre	30000 N/rad
C_s	Longitudinal stiffness of one tyre	50000 N/rad
K_R	Ratios of front roll stiffness to the total roll stiffness	0.552
K_φ	Roll axis torsional stiffness	66185.8 N·m/rad
C_φ	Roll axis torsional damping	3511.6 N·m/rad/sec
ε_r	Road adhesion reduction factor	0.015 s/m
g	Acceleration of gravity	9.81 m/s^2
μ	Nominal friction coefficient between tyre and ground	0.9

In this section, a simulation study is conducted to show the effectiveness of the proposed control system. The simulation maneuver is a single lane change maneuver as shown in Fig. 5. The simulation results are carried out by using an 8DOF nonlinear dynamic vehicle model and a simulation software based on MATLAB and SIMULINK. The vehicle parameters employed for computer simulations are given in Table 1. The initial longitudinal velocity is 30m/s.

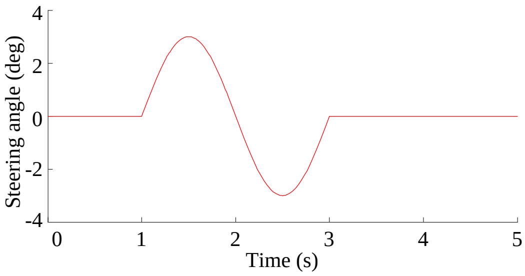

Fig. 5: Steering input angle

In order to verify the effectiveness of the distribution strategy of the longitudinal force, the simulation, without considering actuator dynamics on a day pavement, was conducted. The simulation results were compared with the uncontrolled system and a common DYC system of which the yaw moment are generated by the differential braking. The comparison results are shown in Fig. 6. The proposed DYC controller is named ‘New DYC’ (NDYC), the common DYC is named ‘Common DYC’ (CDYC), and uncontrolled system is named ‘Uncontrol’.

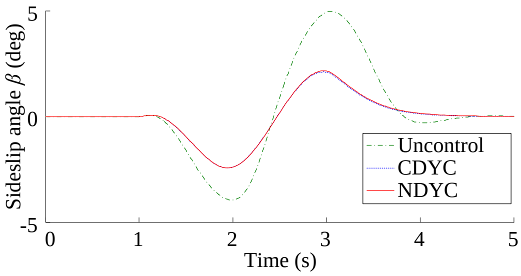

(a) Sideslip angle

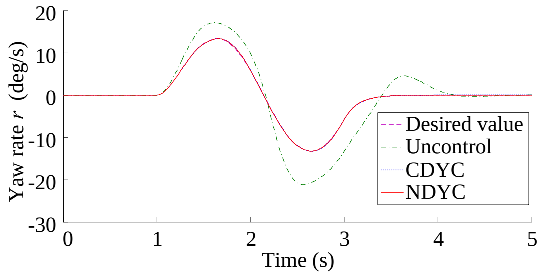

(b) Yaw rate

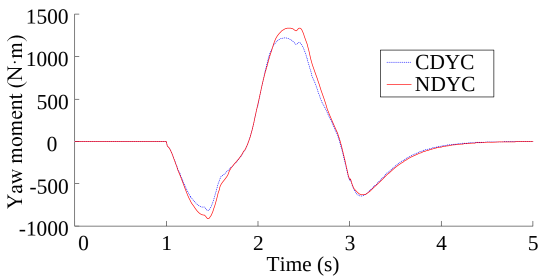

(c) Yaw moment

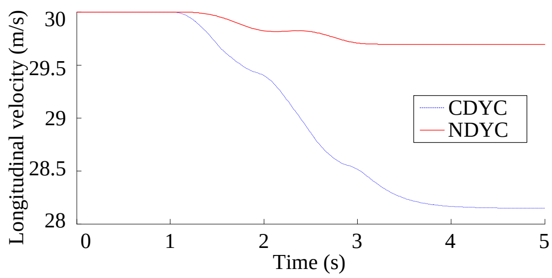

(d) Longitudinal velocity

Fig. 6: Comparison of vehicle responses with different control systems

From Fig. 6(a) and (b), NDYC and CDYC system is obviously better than uncontrolled system. In Fig. 6(c), the required additional yaw moment of NDYC and CDYC is almost equal. But, Fig. 6(d) shows the change of longitudinal velocity under CDYC is even higher. This means that NDYC has more comfortable driving condition and greater potential to stabilize the vehicle. Because when the vehicle’s speed decreases, the vehicle is easier to be stabilized. Therefore, the driving comfort and stability of NDYC is better than CDYC.

Without considering the influence of actuators and sensors on the design of the traditional controllers and with the bad influence on the stability of the control system from the pure time delay of actuators and sensors, the effects of delay of actuators dynamics and sensors are studied in this section. For simplicity, the pure time delay of the actuators dynamics and sensors are considered in the item $e^{-\vartheta s}$. Compared with the pure time delay link, the first-order link of the actuators has less effect on the stability of the control system. Thus, in this section, the first-order link is not studied. The first-order delay time τ_a is 0.05s. The simulation results are shown in Fig. 7 and Fig. 8 The NDYC system has taken into consideration the pure time delay’s influence in the design process, and also contains the Smith predictor. The CYDC system has not considered the pure time delay’s influence and excludes the Smith predictor.

Fig. 7(a) and (b) show when the pure time delay ϑ is 0.01, both CDYC and NDYC system track the desired value well and stabilize the vehicle. However, from Fig. 7(c), the yaw moment of CDYC has an obvious fluctuation, and the yaw moment of NDYC is smooth. From Fig. 8, when the pure time delay ϑ is 0.02, NDYC system is obviously better than CDYC. Fig. 8(b) shows that the yaw rate of

CDYC has no convergence. Fig. 8(c) shows that the yaw moment of CDYC has a severe fluctuation. The NDYC still can work very well.

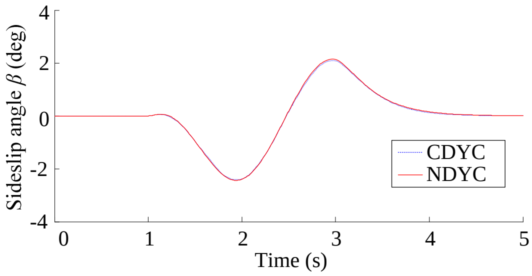

(a) Sideslip angle

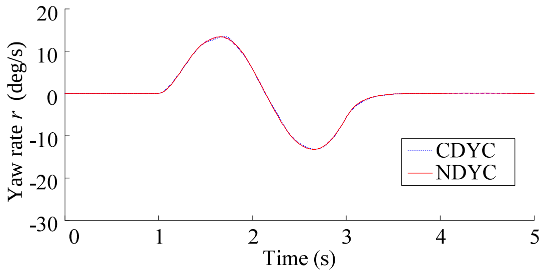

(b) Yaw rate

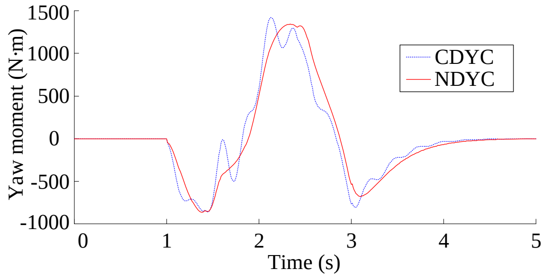

(c) Yaw moment

Fig.7: Comparison of vehicle responses with different control systems at pure time delay ϑ = 0.01s.

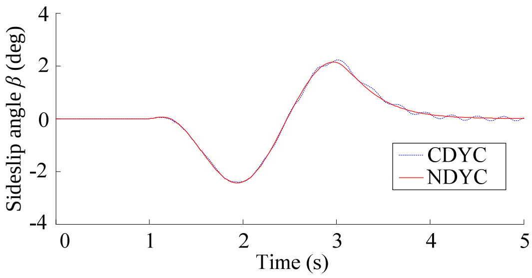

(a) Sideslip angle

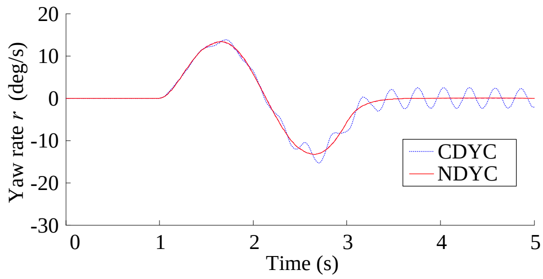

(b) Yaw rate

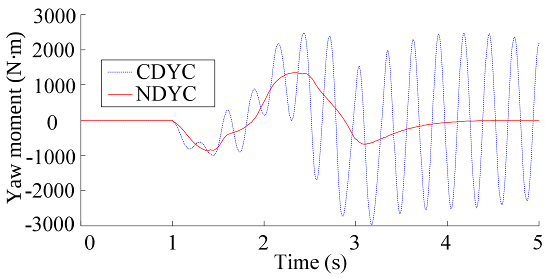

(c) Yaw moment

Fig.8: Comparison of vehicle responses with different control systems at pure time delay ϑ = 0.02s.

5 Conclusion

The stability control system is proposed based on a novel longitudinal force distribution strategy and Smith predictor. A DYC controller using sliding-mode technique is designed to follow the desired yaw rate. According to the yaw moment calculated by the DYC controller, a novel Distributer is designed to distribute the driving or braking torque on each wheel and realizes the yaw moment control. In order to solve the influence of the actuators and sensors/observers on the stability of the control system, a Smith predictor based on the linear 2DOF vehicle model is designed. The simulation results show that the proposed control algorithm can improve vehicle's handling and stability effectively compared with CDYC and uncontrolled system. The distribution strategy of the longitudinal force can meet the demand of the yaw moment, reduce the interference of the longitudinal velocity effectively, and enhance the vehicle driving comfort. Meanwhile, Smith predictor effectively reduces the effect of the delay on the system stability and improves the system stability margin.

Acknowledgements
This work was supported by the National Natural Science Foundation of China (Grant No. 61106029), the Fundamental Research Funds for the Central Universities (Grant No. NS2014020), the Research Fund for the Doctoral Program of Higher Education (Grant No. 20133218120028), and the Foundation of Graduate Innovation Center in NUAA (Grant No. kfjj201405).

References:

[1] J. Gu, M. Ouyang, D. Lu, J. Li and L. Lu, "Energy efficiency optimization of electric vehicle driven by in-wheel motors." *International Journal of Automotive Technology*, Vol. 14, No. 5, pp. 763-772, 2013.
[2] C. Geng, L. Mostefai, M. Denaï and Y. Hori, "Direct yaw-moment control of an in-wheel-motored electric vehicle based on body slip angle fuzzy observer." *Industrial Electronics, IEEE Transactions on*, Vol. 56, No. 5, pp. 1411-1419, 2009.
[3] B. C. Chen and C. C. Kuo, "Electronic stability control for electric vehicle with four in-wheel motors." *International Journal of Automotive Technology*, Vol. 15, No. 4, pp. 573-580, 2014.
[4] R. de Castro, M. Tanelli, R. E. Araújo and S. M. Savaresi, "Minimum-time manoeuvring in electric vehicles with four wheel-individual-motors." *Vehicle System Dynamics*, pp. 1-23, 2014 (ahead-of-print).
[5] R. Rajamani, "*Vehicle dynamics and control*." Springer, 2011.
[6] M. Nagai, Y. Hirano and S. Yamanaka, "Integrated control of active rear wheel steering and direct yaw moment control." *Vehicle System Dynamics*, vol. 27, no. 5-6, pp. 357-370, 1997.
[7] B. L. Boada, M. J. L. Boada and V. Diaz "Fuzzy-logic applied to yaw moment control for vehicle stability." *Vehicle System Dynamics*, vol. 43, no. 10, pp. 753-770, 2005.
[8] A. H. Niasar, H. Moghbeli and R. Kazemi, "Yaw moment control via emotional adaptive neuro-fuzzy controller for independent rear wheel drives of an electric vehicle." *Control Applications, 2003. CCA 2003. Proceedings of 2003 IEEE Conference on. IEEE*, vol. 1, pp. 380-385, 2003.
[9] M. Abe, Y. Kano, K. Suzuki and Y. Furukawa, "Side-slip control to stabilize vehicle lateral motion by direct yaw moment." *JSAE review*, vol. 22, no. 4, pp. 413-419, 2001.
[10] Y. Chen, J. K. Hedrick and K. Guo. "A novel direct yaw moment controller for in-wheel motor electric vehicles." *Vehicle System Dynamics*, vol. 51, no. 6, pp. 925-942, 2013.
[11] A. Roshanbin and M. Naraghi, "Vehicle integrated control-an adaptive optimal approach to distribution of tire forces." *Networking, Sensing and Control, 2008. ICNSC 2008. IEEE International Conference on. IEEE*, pp. 885-890, 2008.
[12] D. E. Smith and J. M. Starkey, "Effects of model complexity on the performance of automated vehicle steering controllers: model development, validation and comparison." *Vehicle System Dynamics*, vol. 24, no. 2, pp. 163-181, 1995.
[13] E. Esmailzadeh, G. R. Vossoughi and A. Goodarzi, "Dynamic modeling and analysis of a four motorized wheels electric vehicle." *Vehicle System Dynamics*, vol. 35, no. 3, pp. 163-194, 2001.
[14] H. Dugoff, P.S. Fancher and L. Segel, "An analysis of tire traction properties and their influence on vehicle dynamic performance." *SAE 700377*, pp. 1219–1243, 1970.
[15] F. Yu and Y. Lin. "*Vehicle System Dynamics*." Beijing: China Machine Press, 2008. (in Chinese)
[16] H. Zhou and Z. Liu, "Vehicle yaw stability-control system design based on sliding mode and backstepping control approach." *Vehicular Technology, IEEE Transactions on*, vol. 59, no. 7, pp. 3674-3678, 2010.
[17] S. Majhi and D. P. Atherton, "Modified Smith predictor and controller for processes with time delay." *IEEE Proceedings-Control Theory and Applications*, vol. 146, no. 5, pp. 359-366, 1999.
[18] I. Kaya, "IMC based automatic tuning method for PID controllers in a Smith predictor configuration." *Computers & chemical engineering*, vol. 28, no. 3, pp. 281-290, 2004.